

PROPERTIES OF TYPE II PLATEAU SUPERNOVA SNLS-04D2DC: MULTICOLOR LIGHT CURVES OF SHOCK BREAKOUT AND PLATEAU

N. TOMINAGA^{1,2,3}, S. BLINNIKOV^{4,2}, P. BAKLANOV^{4,5}, K. NOMOTO^{2,6}

Accepted for publication in the Astrophysical Journal Letters on 21 September 2009.

ABSTRACT

Shock breakout is the brightest radiative phenomenon in a Type II supernova (SN). Although it was predicted to be bright, the direct observation is difficult due to the short duration and X-ray/ultraviolet-peaked spectra. First entire observations of the shock breakouts of Type II Plateau SNe (SNe IIP) were reported in 2008 by ultraviolet and optical observations by the *GALEX* satellite and supernova legacy survey (SNLS), named SNLS-04D2dc and SNLS-06D1jd. We present multicolor light curves of a SN IIP, including the shock breakout and plateau, calculated with a multigroup radiation hydrodynamical code STELLA and an evolutionary progenitor model. The synthetic multicolor light curves reproduce well the observations of SNLS-04D2dc. This is the first study to reproduce the ultraviolet light curve of the shock breakout and the optical light curve of the plateau consistently. We conclude that SNLS-04D2dc is the explosion with a canonical explosion energy 1.2×10^{51} ergs and that its progenitor is a star with a zero-age main-sequence mass $20M_{\odot}$ and a presupernova radius $800R_{\odot}$. The model demonstrates that the peak apparent *B*-band magnitude of the shock breakout would be $m_B \sim 26.4$ mag if a SN being identical to SNLS-04D2dc occurs at a redshift $z = 1$, which can be reached by 8m-class telescopes. The result evidences that the shock breakout has a great potential to detect SNe IIP at $z \gtrsim 1$.

Subject headings: shock waves — radiative transfer — supernovae: general — supernovae: individual (SNLS-04D2dc) — stars: evolution

1. INTRODUCTION

In a supernova (SN) explosion, an outward shockwave formed in an inner layer propagates through the stellar envelope. When the shock emerges from the stellar surface, a hot fire ball suddenly appears and flashes in soft X-ray or ultraviolet (UV). The flash has a quasi-blackbody spectrum ($T \sim 10^6 - 10^5$ K) and lasts a few seconds to ~ 1 days, depending on an ejecta mass M_{ej} , explosion energy E , and presupernova radius R_{preSN} (e.g., Matzner & McKee 1999). The phenomenon is called “shock breakout” having been theoretically predicted (e.g., Klein & Chevalier 1978).

Owing to the short duration and X-ray/UV-peaked spectra, it is difficult to observe directly the shock breakout. The first detection of shock breakout was reported for nearby Type II-peculiar SN 1987A (Catchpole et al. 1987; Hamuy et al. 1988), but it was only a detection of a rapid decline presumed to be a shock breakout tail. Although the detections of shock breakout tails were occasionally reported for Type IIb SN 1993J (Richmond et al.

1994) and Type Ib SN 1999ex (Stritzinger et al. 2002), there were no observations of shock breakouts from the rising part or with the X-ray or UV light.

First entire observations of the shock breakouts were reported in 2008. A first example is an X-ray observation of Type Ib SN 2008D which fortunately appeared in the same galaxy as SN 2007uy during the observation by the *Swift* satellite (Soderberg et al. 2008; Mazzali et al. 2008; Modjaz et al. 2009; Malesani et al. 2009). Second examples are Type II plateau SNe (SNe IIP) SNLS-04D2dc ($z = 0.185$, Schawinski et al. 2008; Gezari et al. 2008) and SNLS-06D1jd ($z = 0.324$, Gezari et al. 2008). They were caught coincidentally in the UV Deep Imaging Survey by the *GALEX* satellite (Morrissey et al. 2005, 2007) at the location where supernova legacy survey (SNLS, Astier et al. 2006) found SN candidates.

Since SNe IIP are the most common among core-collapse types of SNe (e.g., Mannucci et al. 2008) and their shock breakouts are suggested to be so bright as to be detected even at $z \gtrsim 1$ (e.g., Chugai et al. 2000), it is important to develop a way to derive SN properties from the shock breakouts. Therefore, we calculate multicolor light curves (LCs), including a shock breakout and plateau, of SN IIP based on an evolutionary progenitor model with a multigroup radiation hydrodynamics code STELLA (Blinnikov et al. 1998, 2000, 2006). The synthetic LCs are compared with the multicolor observations of SN IIP SNLS-04D2dc (R.A. = $10^{\text{h}}00^{\text{m}}16.7^{\text{s}}$, decl. = $+02^{\circ}12'18.52''$ [J2000.0]).⁷ We first present a multicolor LC model reproducing well the shock breakout and plateau consistently and constrain SN and progeni-

⁷ We focus on SNLS-04D2dc because SNLS-06D1jd has sparse UV observations with relatively low signal-to-noise ratio.

¹ Department of Physics, Faculty of Science and Engineering, Konan University, 8-9-1 Okamoto, Kobe, Hyogo 658-8501, Japan; tominaga@konan-u.ac.jp

² Institute for the Physics and Mathematics of the Universe, University of Tokyo, 5-1-5 Kashiwanoha, Kashiwa, Chiba 277-8569, Japan

³ Optical and Infrared Astronomy Division, National Astronomical Observatory, 2-21-1 Osawa, Mitaka, Tokyo 181-8588, Japan

⁴ Institute for Theoretical and Experimental Physics (ITEP), Moscow 117218, Russia; sergei.blinnikov@itep.ru, baklanovp@gmail.com

⁵ Max-Planck-Institute for Astrophysics, Karl-Schwarzschild-Str. 1, 85741 Garching, Germany

⁶ Department of Astronomy, School of Science, University of Tokyo, Bunkyo-ku, Tokyo 113-0033, Japan; nomoto@astron.s.u-tokyo.ac.jp

tor properties. Furthermore, based on the multicolor LC model, we present an apparent B -band light curve of a shock breakout of a SN being identical to SNLS-04D2dc at $z = 1$.

In § 2, the applied models and the radiation hydrodynamics calculations are described. In § 3, the multicolor LCs of SNLS-04D2dc are compared with the synthetic LCs. In § 4, conclusion and discussion are presented.

2. METHODS & MODELS

We apply the multigroup spherical radiation hydrodynamics code STELLA (Blinnikov et al. 1998, 2000, 2006). STELLA adopts variable Eddington factors, a gray transfer of γ -ray from radioactive nuclei, LTE ionization states, and a multigroup expansion opacity and solves the time-dependent equations implicitly for the angular moments of intensity averaged over fixed frequency bands (for details, see Blinnikov et al. 2006 and references therein). Multigroup radiative transfer is coupled with hydrodynamics, which enables to acquire the spectral energy distributions (SEDs) self-consistently. The color temperature of a SN is estimated from a black-body fitting of the SED. In this Letter we adopt 100 frequency bins dividing logarithmically from $\lambda = 1 \text{ \AA}$ to $5 \times 10^4 \text{ \AA}$; the large number of frequency bins allows to describe accurately a non-equilibrium continuum radiation.

A progenitor model is a non-rotating solar-metallicity star constructed by a stellar evolution calculation (Umeda & Nomoto 2005). The calculation includes a metallicity-dependent mass loss (Kudritzki 2000) and thus the presupernova model has a self-consistent R_{preSN} , luminosity, temperature, envelope mass, and total mass.⁸ Since the shock breakout and plateau depend on M_{ej} , E , and R_{preSN} (e.g., Eastman et al. 1994; Matzner & McKee 1999), our calculation achieves self-consistent multicolor LCs from the shock breakout to plateau and tail. In this Letter we present a SN explosion of a star with a zero-age main-sequence mass $M_{\text{ZAMS}} = 20M_{\odot}$ having a presupernova mass $M_{\text{preSN}} = 18.4M_{\odot}$, H envelope mass $M_{\text{env}} = 13.4M_{\odot}$, and presupernova radius $R_{\text{preSN}} = 800R_{\odot}$. An extensive investigation will be presented in a forthcoming paper.

3. COMPARISONS WITH OBSERVATIONS

Schawinski et al. (2008) and Gezari et al. (2008) found a UV brightening at the SNLS-04D2dc position which lasts several days from ~ 15 days before the first SNLS observation. Although the optical observation of the shock breakout is not available, the UV-optical LCs of the shock breakout and plateau can be compared with the synthetic multicolor LCs. We assume the date of shock breakout to be 2453062.2 JD ($t = 0$) and compare the model and observations with reference to the date. In this Letter the epochs are described in the observer frame.

The multigroup spherical radiation hydrodynamics calculation provides wavelength- and time-dependent fluxes at the SN surface. When a SN is observed from a given direction, lights from different parts of the SN surface are radiated at different time and at different radii (for details, see Klein & Chevalier 1978; Imshennik et al. 1981;

⁸ We note that the presupernova progenitor structure depends on the treatments of physics, e.g., rotation, mass loss, mixing length, and overshooting (e.g., Limongi & Chieffi 2006).

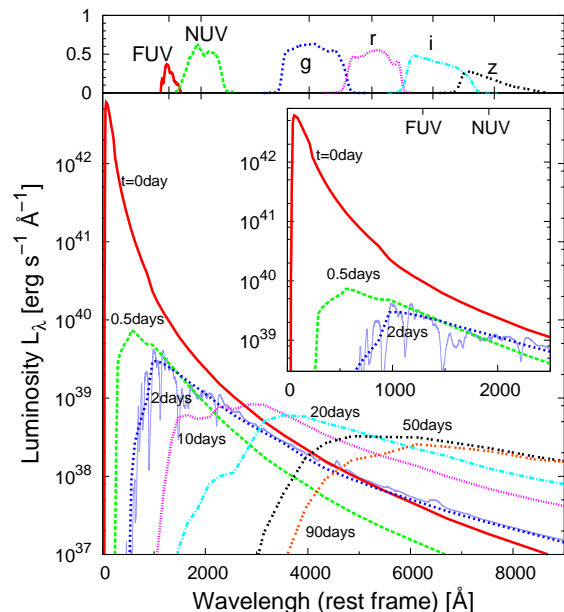


FIG. 1.— *Top*: Sensitivity curves of multicolor bands (red: FUV-band, green: NUV-band, blue: g -band, magenta: r -band, cyan: i -band, and black: z -band). For illustration purpose, each filter band is blueshifted to the rest frame to compensate for $z = 0.185$. *Bottom*: Evolution of intrinsic SEDs of a SN IIP model with $M_{\text{ZAMS}} = 20M_{\odot}$ and $E = 1.2 \times 10^{51}$ ergs at $t = 0$ day (red), 0.5 days (green), 2 days (blue), 10 days (magenta), 20 days (cyan), 50 days (black), and 90 days (orange). A synthetic non-LTE spectrum is also shown (violet, Gezari et al. 2008). The inset enlarges the UV emission at $t = 0, 0.5$, and 2 days and the non-LTE spectrum.

Ensmann & Burrows 1992; Blinnikov et al. 2002, 2003). Thus, we take into account a light travel time correction and limb darkening in the Eddington approximation (Klein & Chevalier 1978). Figure 1 shows corrected wavelength-dependent luminosities L_{λ} for a SN IIP model with $M_{\text{ZAMS}} = 20M_{\odot}$ and $E = 1.2 \times 10^{51}$ ergs.

The SED at $t = 2$ days is compared with synthetic non-LTE spectrum (55.6 hr, Gezari et al. 2008; see also Dessart & Hillier 2005) which gives similar optical color. Although the epochs are different because of adopting different progenitor models, the UV SED and spectrum derived from the independent calculations are distinctly consistent. The consistency justifies both theoretical calculations.

In order to predict multicolor observations from the multicolor theoretical model, the model lights are diluted,⁹ redshifted, reddened, and then convolved with the sensitivities of the satellite and telescope (*GALEX*: Morrissey et al. 2005, 2007, the MegaPrime/MegaCam on the Canada-France-Hawaii Telescope (CFHT) for SNLS: Astier et al. 2006). For illustration purpose, the sensitivity curves blueshifted to the rest frame to compensate for $z = 0.185$ are shown in the top panel of Figure 1. In this Letter the bands are described in the observer frame.

3.1. Ultraviolet light curves of shock breakout

The UV light allows for direct observations of the shock breakout but is strongly reduced by extinction. Thus it is crucial to estimate correctly the extinction

⁹ The distance is derived with the five-year result of *Wilkinson Microwave Anisotropy Probe* (Komatsu et al. 2009).

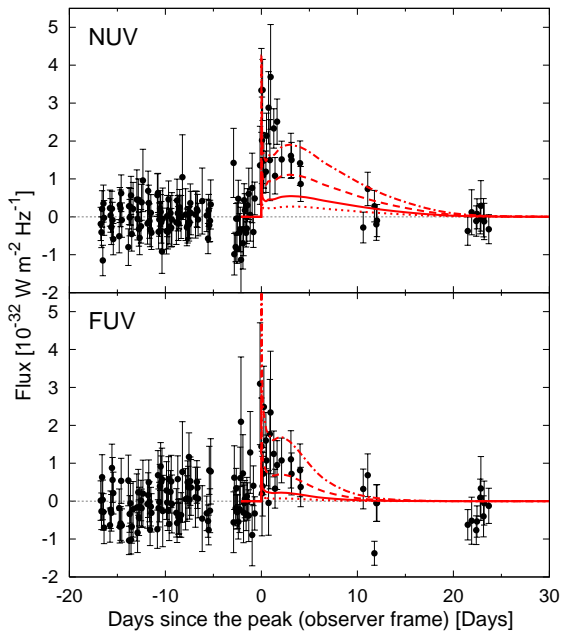


FIG. 2.— Comparison between the NUV (*top*) and FUV (*bottom*) observations (*points*, SNLS-04D2dc, Schawinski et al. 2008) and the SN IIP model without the host galaxy extinction (*dot-dashed line*) and reddened for the host galaxy extinction with $E_{B-V,host} = 0.06$ mag (*dashed line*), 0.14 mag (*solid line*), and 0.22 mag (*dotted line*).

in the host galaxy and our Galaxy. While the color excess of our Galaxy $E_{B-V,Gal}$ is taken from Schlegel et al. (1998, $E_{B-V,Gal} = 0.02$ mag), it is difficult to estimate the color excess and thus extinction of the host galaxy. Schawinski et al. (2008) estimates the color excess of the host galaxy $E_{B-V,host}$ at the SN location from the Balmer decrement as $E_{B-V,host} = 0.14$ mag. However, they caution that the uncertainty of the total extinction is as much as a factor of two and further note that the estimate from the empirical relation of SNe IIP (Nugent et al. 2006) is consistent with both of $E_{B-V,host} = 0.14$ mag and 0.

Assuming the Small Magellanic Cloud (SMC) reddening law for the host galaxy (Pei 1992) and $E_{B-V,host} = 0.14$ mag, the total extinction at the effective wavelengths of the far and near UV (FUV and NUV) filters of the *GALEX* satellite are as large as $A_{FUV} = 2.38$ mag and $A_{NUV} = 1.51$ mag, respectively. Hereafter, we call these values “standard” extinction. Although the values are slightly different from Schawinski et al. (2008), the total extinction integrated over each band depends on the intrinsic spectrum and varies with time as the spectrum changes. The variations of extinction in the UV bands are relatively large; for example, ~ 0.3 mag in the FUV band and ~ 0.1 mag in the NUV band from $t = 0$ to 20 days for the SN IIP model with $M_{ZAMS} = 20M_{\odot}$ and $E = 1.2 \times 10^{51}$ ergs.

Because of the large uncertainty, we assume several values for the color excess of the host galaxy as follows: $E_{B-V,host} = 0$ mag referring to the case of no extinction in the host galaxy, $E_{B-V,host} = 0.06$ mag giving half of the standard extinction in the NUV band, $E_{B-V,host} = 0.14$ mag being the standard extinction, and $E_{B-V,host} = 0.22$ mag giving double of the standard extinction in the NUV band,

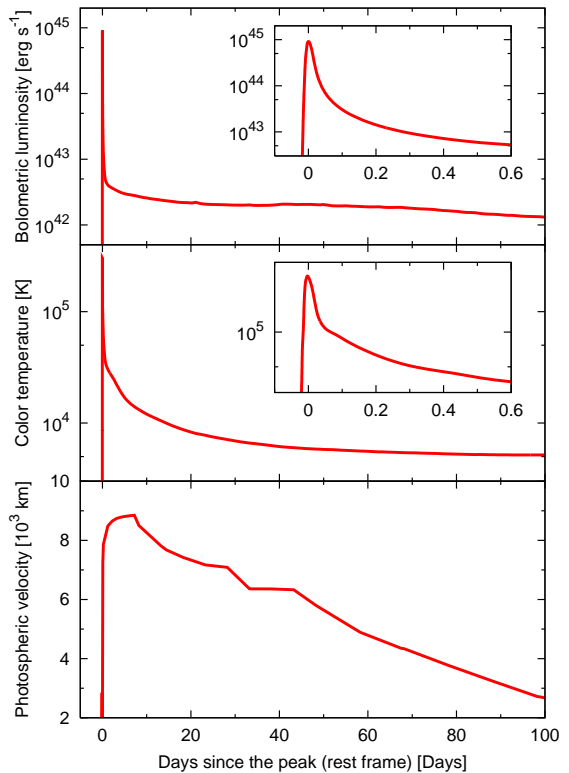


FIG. 3.— Bolometric LC (*top*), color temperature evolution (*middle*), and photospheric velocity evolution (*bottom*) of the SN IIP model (*lines*). The insets in the top and middle panels enlarge the phase of shock breakout.

which lead to $(A_{NUV}, A_{FUV}) = (0.18$ mag, 0.15 mag), (0.75 mag, 1.10 mag), (1.51 mag, 2.38 mag), and (2.27 mag, 3.65 mag), respectively. Here, we assume the SMC reddening law for the host galaxy.

Figure 2 shows comparisons of UV LCs with the model with $M_{ZAMS} = 20M_{\odot}$ and $E = 1.2 \times 10^{51}$ ergs. The model LCs are consistent with the observations within the uncertainty, while they are slightly fainter than the observations for $E_{B-V,host} = 0.14$ mag. The explosion energy of SNLS-04D2dc is consistent with the canonical value of the explosion energies of core-collapse SNe [e.g., SN 1987A: $E = (1.1 \pm 0.3) \times 10^{51}$ ergs, Blinnikov et al. 2000]. Although the ^{56}Ni - ^{56}Co radioactive decay does not contribute to the shock breakout, we expediently assume a canonical ^{56}Ni ejection without mixing to the envelope [the ejected ^{56}Ni mass $M(^{56}\text{Ni}) = 0.07M_{\odot}$, e.g., SN 1987A: Blinnikov et al. 2000], and thus $M_{ej} = 16.9M_{\odot}$ to yield $0.07M_{\odot}$ of ^{56}Ni .

The second peak in the NUV LC at $t \sim 3$ days is reproduced by the model and explained by the shift of the peak wavelength as Schawinski et al. (2008) and Gezari et al. (2008) suggested. The bolometric LC and the evolution of color temperature are shown in Figure 3. Figure 3 also shows the velocity evolution of photosphere defined as a position where the radiation and gas are decoupled. Although the bolometric luminosity declines monotonically after the shock breakout, the radiation energy in the NUV band increases with time because the peak wavelength shifts long (Fig. 1). After the NUV second peak, the color temperature decreases further and the peak wavelength shifts to the optical bands. The shift is caused by not only the decreasing temperature of the SN

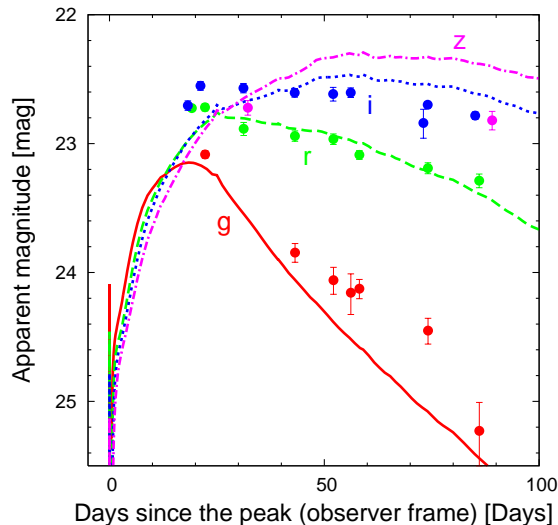


FIG. 4.— Comparison between the SNLS observations (points, SNLS-04D2dc, Schawinski et al. 2008) and the SN IIP model reddened for the host galaxy extinction with $E_{B-V, \text{host}} = 0.14$ mag (lines) (red: g -band, green: r -band, blue: i -band, magenta: z -band in AB magnitude system).

ejecta but also an enhancement of the metal absorption lines due to the low temperature. As a result, the UV luminosity declines monotonically after the NUV second peak. The model also predicts a second peak in the FUV band but the brightening is obscured because of the low signal-to-noise ratio.

3.2. Optical light curves at plateau stage

Thanks to the multigroup radiation hydrodynamics calculations, subsequent evolutions of multicolor lights are obtained and compared with the SNLS optical observations. Figure 4 shows comparisons of the g -, r -, i -, and z -band LCs. Here, we adopt $E_{B-V, \text{host}} = 0.14$ mag and the SMC reddening law for the host galaxy. The total extinction at the effective wavelengths of the g -, r -, i -, and z -band filters of the MegaPrime/MegaCam on CFHT are as large as $A_g = 0.64$ mag, $A_r = 0.47$ mag, $A_i = 0.36$ mag, and $A_z = 0.28$ mag, respectively.

As SED peaks in the g -band at $t \sim 20$ days (Fig. 1), the g -band LC peaks at $t \sim 20$ days. After this epoch, the SED becomes red with time and the blue edge of the SED enters in the g -band. Thus, the g -band LC declines more rapidly than the other optical-band LCs. On the other hand, the r -band LC declines gradually and the decline rate slightly changes at $t \sim 55$ days when the SED peak enters in the r -band. The i - and z -band LCs brighten by $t \sim 60$ days due to the shift of the peak wavelength.

Although the overall multicolor LCs are well reproduced by the model, the z -band model LC is brighter than the observation at $t \sim 90$ days. The discrepancy would be improved if we add more physics to STELLA. STELLA currently has around 1.5×10^5 spectral lines from Kurucz & Bell (1995) and Verner et al. (1996) and a rather poor line list in near infrared, while tens of millions of spectral lines from large Kurucz lists are being included (E. Sorokina, private communication). The expansion of line lists, together with taking into account non-equilibrium effects in an important coolant like Ca II, may influence the z -band flux appreciably

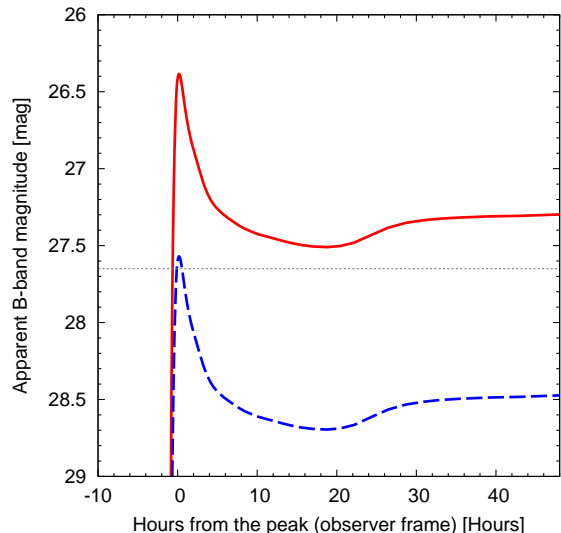


FIG. 5.— Apparent B -band light curve of a shock breakout in AB magnitude system for a SN being identical to SNLS-04D2dc at $z = 1$. We assume $E_{B-V, \text{Gal}} = 0.02$ mag, $E_{B-V, \text{host}} = 0$ (solid line) and 0.14 mag (dashed line), and the SMC reddening law for the host galaxy. A limiting magnitude for a 4σ detection in a hour of integration with SUBARU/Suprime-Cam (Miyazaki et al. 2002) is also shown (dotted line), which is calculated with Subaru Imaging Exposure Time Calculator (http://www.naoj.org/cgi-bin/spcam_tmp.cgi) assuming $0.5''$ seeing, 1.5 arcsec aperture, and 3 days from New Moon.

(Kasen 2006).

No mixing of ^{56}Ni leads to no contribution from the radioactive heating to the LC at $t \lesssim 100$ days, while the radioactive decay could power the LC from the early phases if ^{56}Ni is mixed to the envelope. Because of the lack of observations at $t > 100$ days, $M(^{56}\text{Ni})$ of SNLS-04D2dc cannot be constrained. We note that the available observations can be reproduced equally well even if no ^{56}Ni is ejected.

4. CONCLUSIONS & DISCUSSION

We present a multicolor LC model with the multigroup radiation hydrodynamical code STELLA. The model reproduces the multicolor UV-optical LCs of the shock breakout and plateau of SNLS-04D2dc consistently. Since the shock breakout is more sensitive to E and R_{preSN} than the plateau (Eastman et al. 1994; Matzner & McKee 1999), the SN and progenitor properties are constrained more tightly than only with the plateau observation. We clarify the properties of SNLS-04D2dc: the progenitor is a star with $M_{\text{ZAMS}} = 20M_{\odot}$, $M_{\text{preSN}} = 18.4M_{\odot}$, and $R_{\text{preSN}} = 800R_{\odot}$, and the SN has the canonical explosion energy $E = 1.2 \times 10^{51}$ ergs. Because of no observations at $t > 100$ days, we cannot constrain $M(^{56}\text{Ni})$ of SNLS-04D2dc, while we expediently adopt $M_{\text{ej}} = 16.9M_{\odot}$ and $M(^{56}\text{Ni}) = 0.07M_{\odot}$.

The second peak of the NUV LC is reproduced by the shift of the peak wavelength, in spite of the monotonic decline of the bolometric LC. Although the signal-to-noise ratio of the FUV LC is quite low, the model is also in an agreement with the FUV LC. The consistency supports the origin of the NUV second peak. When only the monotonic light curve is obtained, only two observational quantities, i.e., flux and duration, are available and the three properties characterizing the shock breakout, M_{ej} ,

R_{preSN} , and E , are degenerated. The multicolor observation enables us to constrain the color temperature and thus to resolve the degeneracy. In order to clarify the SN properties in detail, it is required to employ the multi-group radiation hydrodynamical calculations because the spectra of the shock breakout slightly deviate from the blackbody.

The successful reproduction of UV-optical LCs of SNLS-04D2dc and the consistency with the non-LTE spectral calculation justify the multigroup radiation hydrodynamics calculation with STELLA and indicate that the calculations are capable of predicting the multicolor observations of the shock breakout and plateau of SNe IIP. If a SN being identical to SNLS-04D2dc takes place at $z = 1$ in the direction with $E_{B-V, \text{Gal}} = 0.02$ mag, the SN brightness will be $m_B \sim 26.4$ mag without the host galaxy extinction or $m_B \sim 27.6$ mag with the host galaxy extinction with $E_{B-V, \text{host}} = 0.14$ mag and the SMC reddening law (Fig. 5). It is bright enough to be detected with 8m-class telescopes. The result envisages that future deep and wide surveys by, e.g., SkyMapper, Panoramic Survey Telescope and Rapid Response System (Pan-STARRS), Large Synoptic Survey Telescope (LSST), and SUBARU/Hyper Suprime-Camera (HSC), will find a large number of shock breakouts. The large sample will import totally-new knowledge about cosmic evolution histories, e.g., a core-collapse SN rate and a star formation rate, at $z \gtrsim 1$. Therefore, although the detections of Type II In SNe at $z > 2$ are recently reported (Cooke et al. 2009), we still emphasize a great potential of shock breakouts for direct detection of the most common core-collapse SNe, SNe IIP, at $z \gtrsim 1$.

Finally, we point out that the estimate of the host galaxy extinction is crucial to estimate the intrinsic luminosity of shock breakout. This is because the shock breakout of SN IIP emits the radiation energy mainly in UV easily reduced by the interstellar extinction. With the use of the sensitiveness, if the observations of shock breakout, plateau, and tail are available with high signal-to-noise ratios, finding a set of a SN model and extinction, which consistently reproduces the observations, might provide a new constraint on the host galaxy extinction.

We thank Kevin Schawinski and the co-authors of Schawinski et al. (2008) paper and Luc Dessart and the co-authors of Gezari et al. (2008) paper for kindly providing the data of FUV observations and the data of synthetic non-LTE spectra of the shock breakout, respectively. N.T. appreciates Tomoki Morokuma for helpful discussion. S.B. thanks Katsuhiko Sato and Hitoshi Murayama for hospitality at University of Tokyo during his visits in 2006-2009. N.T. has been supported by the JSPS (Japan Society for the Promotion of Science) Research Fellowship for Young Scientists. The work of S.B. and P.B. in Russia is supported partly by the grant RFBR 07-02-00830-a, by Scientific School Foundation under grants 2977.2008.2, 3884.2008.2, and in Germany by MPA guest program. This research has been supported in part by World Premier International Research Center Initiative, MEXT, Japan, and by the Grant-in-Aid for Scientific Research of the JSPS (18104003, 20540226, 21840055) and MEXT (19047004, 20040004).

REFERENCES

- Astier, P., et al. 2006, *A&A*, 447, 31
 Blinnikov, S. I., Eastman, R., Bartunov, O. S., Popolitov, V. A., & Woosley, S. E. 1998, *ApJ*, 496, 454
 Blinnikov, S., Lundqvist, P., Bartunov, O., Nomoto, K., Iwamoto, K. 2000, *ApJ*, 532, 1132
 Blinnikov, S. I., Nadyozhin, D. K., Woosley, S. E., and Sorokina, E. I. 2002, *Nuclear Astrophysics*, ed. W. Hillebrandt & E. Müller (Garching: Max-Planck-Institut für Astrophysik), 144
 Blinnikov, S., Chugai, N., Lundqvist, P., Nadyozhin, D., Woosley, S., and Sorokina, E. 2003, *From Twilight to Highlight: The Physics of Supernovae*, ed. W. Hillebrandt & B. Leibundgut (New York: Springer), 23
 Blinnikov, S. I., Röpke, F. K., Sorokina, E. I., Gieseler, M., Reinecke, M., Travaglio, C., Hillebrandt, W., & Stritzinger, M. 2006, *A&A*, 453, 229
 Catchpole, R. M., et al. 1987, *MNRAS*, 229, 15
 Cooke, J., Sullivan, M., Barton, E. J., Bullock, J. S., Carlberg, R. G., Gal-Yam, A., & Tollerud, E. 2009, *Nature*, 460, 237
 Chugai, N. N., Blinnikov, S. I., Lundqvist, P. 2000, *Mem. Soc. Astron. Italiana*, 71, 383
 Dessart, L., & Hillier, D. J. 2005, *A&A*, 437, 667
 Eastman, R. G., Woosley, S. E., Weaver, T. A., & Pinto, P. A. 1994, *ApJ*, 430, 300
 Ensmann, L., & Burrows, A. 1992, *ApJ*, 393, 742
 Gezari, S., et al. 2008, *ApJ*, 683, L131
 Hamuy, M., Suntzeff, N. B., Gonzalez, R., Martin, G. 1988, *AJ*, 95, 63
 Imshennik, V. S., Nadezhin, D. K., and Utrobin, V. P. 1981, *Ap&SS*, 78, 105
 Kasen, D. 2006, *ApJ*, 649, 939
 Klein, R. L., & Chevalier, R. A. 1978, *ApJ*, 223, L109
 Komatsu, E., et al. 2009, *ApJS*, 180, 330
 Kudritzki, R.-P. 2000, *The First Stars*, ed. A. Weiss, T. G. Abel, & V. Hill (Berlin: Springer), 127
 Kurucz, R. L., & Bell, B. 1995, *Atomic Line Data Kurucz CD-ROM No. 23* (Cambridge: Smithsonian Astrophysical Observatory)
 Limongi, M., & Chieffi, A. 2006, *ApJ*, 647, 483
 Mannucci, F., Maoz, D., Sharon, K., Botticella, M. T., Della Valle, M., Gal-Yam, A., & Panagia, N. 2008, *MNRAS*, 383, 1121
 Malesani, D., et al. 2009, *ApJ*, 692, L84
 Matzner, C. D. & McKee, C. F. 1999, *ApJ*, 510, 379
 Mazzali, P. A., et al. 2008, *Science*, 321, 1185
 Miyazaki, S., et al. 2002, *PASJ*, 54, 833
 Modjaz, M., et al. 2009, *ApJ*, 702, 226
 Morrissey, P., et al. 2005, *ApJ*, 619, L7
 Morrissey, P., et al. 2007, *ApJS*, 173, 682
 Nugent, P., et al. 2006, *ApJ*, 645, 841
 Pei, Y. C. 1992, *ApJ*, 395, 130
 Richmond, M. W., Treffers, R. R., Filippenko, A. V., Paik, Y., Leibundgut, B., Schulman, E., & Cox, C. V. 1994, *AJ*, 107, 1022
 Schlegel, D. J., Finkbeiner, D. P., & Davis, M. 1998 *ApJ*, 500, 525
 Schawinski, K., et al. 2008, *Science*, 321, 223
 Soderberg, A.M., et al. 2008, *Nature*, 453, 469
 Stritzinger, M., et al. 2002, *AJ*, 124, 2100
 Umeda, H. & Nomoto, K. 2005, *ApJ*, 619, 427
 Verner, D. A., Verner, E. M., & Ferland, G. J. 1996, *Atomic Data Nucl. Data Tables*, 64, 1